Development 136, 3109-3119 (2009) doi:10.1242/dev.039412

Myosin II regulation during *C. elegans* embryonic elongation: LET-502/ROCK, MRCK-1 and PAK-1, three kinases with different roles

Christelle Gally, Frédéric Wissler, Hala Zahreddine, Sophie Quintin, Frédéric Landmann* and Michel Labouesse†

Myosin II plays a central role in epithelial morphogenesis; however, its role has mainly been examined in processes involving a single cell type. Here we analyze the structure, spatial requirement and regulation of myosin II during *C. elegans* embryonic elongation, a process that involves distinct epidermal cells and muscles. We developed novel GFP probes to visualize the dynamics of actomyosin remodeling, and found that the assembly of myosin II filaments, but not actin microfilaments, depends on the myosin regulatory light chain (MLC-4) and essential light chain (MLC-5, which we identified herein). To determine how myosin II regulates embryonic elongation, we rescued *mlc-4* mutants with various constructs and found that MLC-4 is essential in a subset of epidermal cells. We show that phosphorylation of two evolutionary conserved MLC-4 serine and threonine residues is important for myosin II activity and organization. Finally, in an RNAi screen for potential myosin regulatory light chain kinases, we found that the ROCK, PAK and MRCK homologs act redundantly. The combined loss of ROCK and PAK, or ROCK and MRCK, completely prevented embryonic elongation, but a constitutively active form of MLC-4 could only rescue a lack of MRCK. This result, together with systematic genetic epistasis tests with a myosin phosphatase mutation, suggests that ROCK and MRCK regulate MLC-4 and the myosin phosphatase. Moreover, we suggest that ROCK and PAK regulate at least one other target essential for elongation, in addition to MLC-4.

KEY WORDS: Actin, Non-muscle myosin II, Morphogenesis, Phosphorylation, Rho kinase, *C. elegans*

INTRODUCTION

Morphogenesis is an essential feature of embryonic development, during which cells change their overall shape to build tubular organs, extend cell sheets or organize into specific patterns. These changes depend on the organization of the cytoskeleton as well as on its dynamic behavior. Characterization of different morphogenetic processes has revealed the central role played by myosin II and its regulators, the Rho-binding kinase (ROCK) and myosin phosphatase (Conti and Adelstein, 2008; Quintin et al., 2008).

Myosin II is an hexamer composed of two myosin heavy chains, two essential light chains and a pair of regulatory light chains (RMLCs), which converts chemical energy into mechanical force (Conti and Adelstein, 2008). Its activity is regulated in part through phosphorylation of the RMLC by serine/threonine kinases, in particular by ROCK (Somlyo and Somlyo, 2003). Although the importance of myosin II in morphogenesis is undisputed, its spatial organization and specific mechanism of activation have seldom been examined in vivo. Furthermore, its role has so far been documented mainly in morphogenetic processes involving a homogenous cell population in which all cells behave similarly (Quintin et al., 2008).

As an example of morphogenesis, we study *C. elegans* embryonic elongation, during which a bean-shaped embryo is changed into a worm-shaped larva. This process is driven by coordinated shape changes of epidermal cells that lead to a decrease in circumference and a 4-fold increase in length (referred to here as the 4-fold stage) (Priess and Hirsh, 1986). The epidermis is composed of three major cell groups, namely dorsal, ventral and lateral seam cells, with distinct anatomical properties: (1) dorsal and ventral cells, but not lateral seam cells, are in contact with muscles; and (2) most dorsal cells form a syncytium at the 1.5-fold stage (Chisholm and Hardin, 2005).

Treatment of embryos with cytochalasin D established that actin microfilaments (MFs) present in epidermal cells are crucial for elongation (Priess and Hirsh, 1986). Genetic analysis revealed that mutations affecting MLC-4 (RMLC), NMY-1 (one of the two myosin II heavy chains) or LET-502 (ROCK) induce severe elongation defects (Piekny et al., 2003; Shelton et al., 1999; Wissmann et al., 1997). Conversely, mutations affecting MEL-11, the myosin-binding subunit of myosin phosphatase (MYPT), induce embryonic rupture probably due to hypercontraction of the actomyosin cytoskeleton, as an *nmy-1* mutation prevents the rupture of *mel-11* mutants (Piekny et al., 2003). Thus, the pharmacological and genetic analysis performed so far has not examined whether the different epidermal cells play distinct roles in elongation. Furthermore, although genetic analysis would predict that LET-502/ROCK activates MLC-4/RMLC, this has never been formally established during elongation.

C. elegans represents a powerful system to dissect myosin II function and regulation, in part because the organization of actin microfilaments in the epidermis provides exceptional spatial resolution. Here, we use new fluorescent GFP reporters to provide a detailed analysis of how myosin II dynamically functions during embryonic morphogenesis. We identify the myosin essential light chain and characterize its role in elongation. Using tissue-specific promoters and mutant transgenes, we determine in which cells myosin II acts to drive elongation, and dissect the molecular regulation of MLC-4 by phosphorylation. In particular, we examine the potential role of several kinases whose vertebrate orthologs can

IGBMC, CNRS/ INSERM/ UdS, 1 rue Laurent Fries, BP.10142, 67400 Illkirch, France.

*Present address: Molecular, Cell and Developmental Biology, UCSC, Santa Cruz, CA 95064, USA
†Author for correspondence (lmichel@igbmc.fr)

Accepted 13 July 2009

phosphorylate RMLC. We find that ROCK, PAK and MRCK homologs play distinct functions during embryonic elongation, and discuss what their potential targets might be.

MATERIALS AND METHODS

Strains and genetic methods

Control N2 and other animals were propagated at 20°C (unless noted otherwise) (Brenner, 1974). The following strains were used: ML1395, *rrf-3(pk1426) II; mcEx227[lin-26p::ABD$_{VAB-10}$::GFP, rol-6(su1006)]*; EU618, *mlc-4(or253)/qC1[dpy-19(e1259), glp-1(q339)] III*; ML1148, *mlc-4(or253)/qC1;mcEx399[mlc-4p::GFP::mlc-4WT, rol-6(su1006)]*; ML1151, *mlc-4(or253)/qC1;mcEx402[mlc-4p::GFP::mlc-4DD, rol-6(su1006)]*; ML1204, *mlc-4(or253)/qC1;mcEx317[mlc-4p::GFP::mlc-4AA, rol-6(su1006)]*; ML1111, *mlc-4(or253)/qC1;mcEx323[mlc-4p::GFP::mlc-4T17A, rol-6(su1006)]*; ML1114, *mlc-4(or253)/qC1;mcEx326[mlc-4p::GFP::mlc-4S18A, rol-6(su1006)]*; ML1567, *mlc-4(or253)/qC1;mcEx540[ceh-16p::GFP::mlc-4WT, myo-2p::GFP]*; ML1178, *mlc-4(or253)/qC1;mcEx407[elt-3p::GFP::mlc-4WT, myo-2p::GFP]*; ML1568, *mlc-4(or253)/qC1;mcEx541[ceh-16p::GFP::mlc-4WT, elt-3p::GFP::mlc-4WT, myo-2p::GFP]*; HR1157, *let-502(sb118ts) I*; KK332, *mel-11(it26) unc-4(e120) sqt-1(sc13)/mnC1[dpy-10(e128) unc-52(e444)] II*; RB689, *pak-1(ok448) X*; ML1594, *mrck-1(ok586)/nT1[qIs51] V*; ML1312, *mcIs49[mlc-4p::GFP::mlc-4WT, rol-6(su1006)]*; ML1153, *mcIs46[dlg-1::rfp;unc-119(+)]*; ML1310, *mcEx467[lin-26p::ABD$_{VAB-10}$::GFP, myo-2p::GFP]*; ML1152, *mcEx403[mlc-5p::GFP::mlc-5, rol-6(su1006)]*. *pak-1* and *mrck-1* mutations were outcrossed four times. For genetic epistasis experiments, mothers were transferred to fresh plates for 2 hours. Half of this synchronized progeny was observed 5-7 hours after egg laying to determine the terminal phenotype by DIC microscopy (at least 50 embryos were observed). The second half was observed 24 hours after egg laying to quantify embryonic lethality.

RNA interference

RNAi was performed either using the Ahringer-MRC feeding RNA interference (RNAi) library (Kamath et al., 2003), or by injection of double-stranded RNA synthesized from PCR-amplified genomic fragments using a T3 or T7 mMESSAGE mMACHINE Kit (Ambion, Austin, TX, USA).

mlc-5 identification

A feeding RNAi screen was performed on ML1395. L3-L4 stage larvae were placed for 36-40 hours on bacteria producing dsRNA. From these adults, a synchronized egg progeny was observed for elongation and actin organization defects 5 hours after egg laying. Primers used to inactivate *mlc-5* and *mlc-4* were: 5′-AATTAACCCTCACTAAAGGGAGCACATG-GTATTGGGGGAAGTGG-3′ and 5′-AATTAACCCTCACTAAAGGG-AGCACATGGTATTGGGGGAAGTGG-3′; 5′-AATTAACCCTCACTA-AAGGGCTGGGAGAGAGCGAATAAGAAAT-3′ and 5′-AATTAACC-CTCACTAAAGGGCTCATTCTCTCTTTTATCGCCAA-3′, respectively.

Kinase screen

Double-stranded RNA was injected into wild-type and *let-502(sb118ts)* young adults. Injected mothers were stored at the restrictive temperature of 25.5°C overnight and synchronized for egg laying the next morning. The progeny was scored 6-8 hours after egg laying, ~24 hours after dsRNA injection in the mothers.

GFP transgenes

pML1572, *lin-26p::ABD$_{VAB-10}$::GFP*

An RT-PCR fragment corresponding to codons 1-290 of *vab-10a*, which encode two predicted calponin-homology domains (Bosher et al., 2003), was cloned at the *Nhe*I site of a 4 kb *lin-26* promoter fragment [eFGHi construct, see (Landmann et al., 2004)] upstream of *green fluorescent protein* (*GFP*).

pML1517, *lin-26p::ABD$_{VAB-10}$::mcherry*

pML1517 construction was similar to pML1572, except that the *GFP* was replaced by the *mcherry* coding sequence (gift from K. Oegema, Ludwig Institute for Cancer Research – UC San Diego, La Jolla, CA, USA), and a 5 kb *lin-26* promoter was used.

pML1522, *mlc-4p::GFP::mlc-4WT*

The final construct contained 2 kb of the *mlc-4* promoter, the *GFP* coding sequence and the *mlc-4* coding DNA downstream of *GFP*, all assembled in vector pPD97.82, from which the NLS had been removed (gift from A. Fire, Stanford University, Stanford, CA, USA). The different *mlc-4* variants were obtained by PCR-driven mutagenesis onto pML1522 using mutated primers. To generate *ceh-16p*- and *elt-3p*-driven *GFP::mlc-4* constructs, the respective promoter regions of *ceh-16* (2.9 kb) and *elt-3* (1.9 kb) genes were introduced into pML1522 to replace the *mlc-4* promoter.

pML1604, *mlc-5p::GFP::mlc-5*

The final construct contained 2.2 kb of the *mlc-5* promoter, the *GFP* coding sequence and a 2.7 kb region containing *mlc-5* and *taf-9*, which were PCR-amplified and cloned between the *Not*I and *Bam*HI sites of pBSKII$^+$.

pML1580, *mrck-1p::mrck-1::GFP*

The final construct was assembled from a PCR-amplified region including 2.9 kb of the *mrck-1* promoter and most of the coding region, except that the final coding part was substituted with a 1.1 kb PCR cDNA fragment. These fragments were cloned between the *Pst*I and *Kpn*I sites of pPD95.75.

Constructs were injected at 10 ng/μl with either pPD118.33 (*myo-2p::GFP* at 5 ng/μl), pCFJ90 (*myo-2p::mcherry* at 5 ng/μl) or pRF4 (*rol-6(su1006)* at 100 ng/μl) as a selection marker and pBSKII$^+$ (up to 200 ng/μl final concentration).

Laser-scanning and spinning-disk confocal microscopy

Images were captured with a Leica TCS SP5 confocal microscope (using a 63× NA 1.4 Plan Apochromat HCX oil objective) controlled by the Leica LAS AF imaging software. Illumination was via 458 nm and 561 nm lasers. Images were computationally projected using the ImageJ software (ImageJ, NIH, Bethesda, Maryland, USA; http://rsb.info.nih.gov/ij/). Short time-lapse experiments were performed on live embryos using a Leica DMI6000 spinning-disk confocal microscope (100× NA 1.43 Plan Apochromat objective), coupled with an Andor Revolution Spinning Disk System (iXon EMCCD 512 × 512 camera and Yokogawa spinning disk head). For spinning-disk imaging of live embryos, single focal planes are shown.

Embryos were mounted on a 2% agarose pad in M9 buffer and the coverslip was sealed with paraffin oil. For SP5 confocal recordings, oxygen was depleted from the chamber by adding OP50 aerobic bacteria to the medium. This procedure should halt ATP production by the respiratory chain, and might thus indirectly affect protein phosphorylation. For each panel, at least 15 embryos were examined.

mlc-4 rescue experiment

All *mlc-4* constructs were tested in the *mlc-4(or253)/qC1[dpy-19(e1259)glp-1(q339)]* background. Freshly hatched L1 (less than 1.5 hours) were mounted in M9 buffer and photographed using a Zeiss Axioplan microscope under a 10× objective; their length was measured using the ImageJ software. Larvae were recovered from the slide and allowed to grow for 2.5 days at 25°C. The resulting adult homozygous mutants and heterozygotes were discriminated by PCR genotyping. Transgenes injected at 0.5 ng/μl failed to rescue, and transgenes injected at 2.5 ng/μl gave a rescue comparable to 10 ng/μl (not shown).

RESULTS

Actin organization during elongation

Until now the actin cytoskeleton has been visualized by phalloidin staining on fixed embryos, with a high background due to muscle actin staining (Costa et al., 1997; Priess and Hirsh, 1986). To overcome this limitation, we developed a fluorescent probe to visualize actin specifically in the epidermis, which confirmed and extended previous descriptions of MFs. We fused the predicted actin-binding domain (ABD) of the spectraplakin VAB-10 (Bosher et al., 2003) to green fluorescent protein (GFP), and put the resulting construct under the control of the epidermal *lin-26* promoter. The corresponding ABD from the VAB-10 homologs *Drosophila* Shot and mouse MACF1 can bind actin in vitro (Lee and Kolodziej,

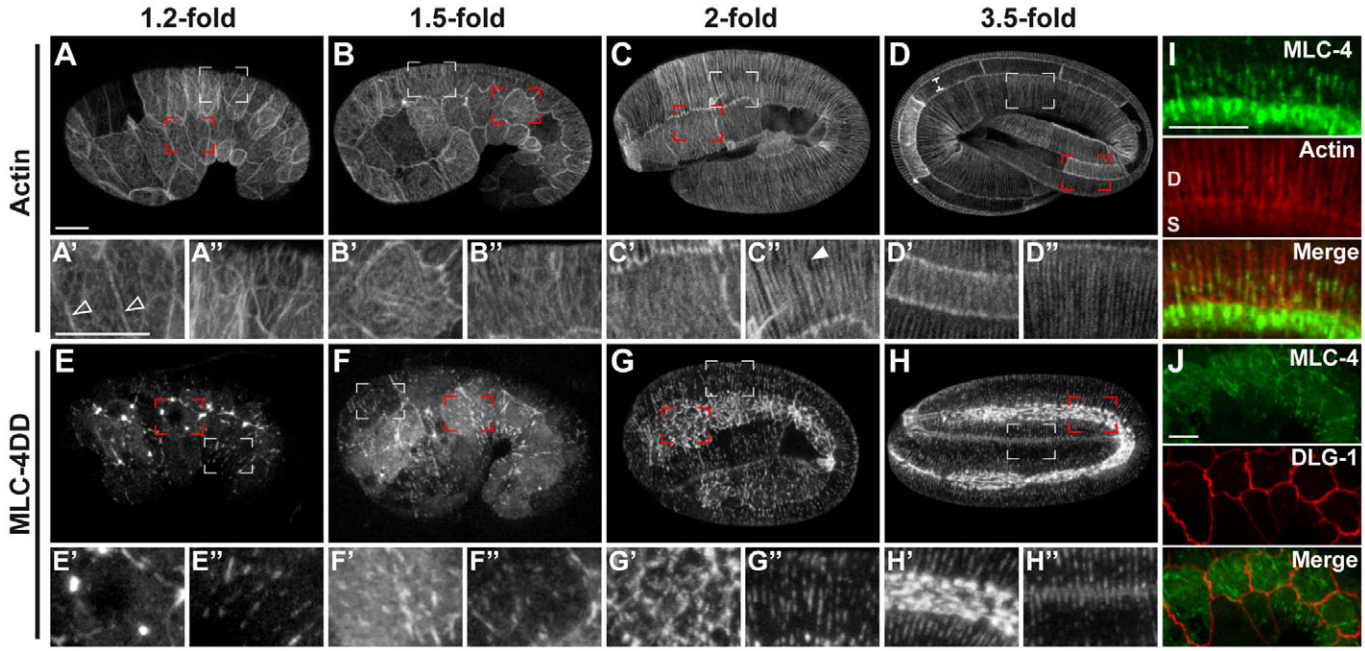

Fig. 1. Actin and MLC-4 colocalize in the epidermis. (**A-H**) Confocal lateral projections of *C. elegans* embryos expressing the ABD_{VAB-10}::GFP construct (A-D) to visualize actin, or the GFP::MLC-4DD construct (E-H). 1.2-fold (A,E), 1.5-fold (B,F), 2-fold (C,G) and 3.5-fold (D,H) stage embryos. Dotted line in D indicates the width of the seam cells. High magnifications show areas marked by open red rectangles (**A′-H′**; seam cells) and white rectangles (**A″-H″**; DV cells). Open arrowheads in A, membranes; arrowhead in C″, discontinuities in actin bundles at the 2-fold stage. (**I**) Coexpression of GFP::MLC-4DD (green) and ABD_{VAB-10}::mCherry (red), showing the overlap of both markers in a 3.5-fold embryo. (**J**) Coexpression of GFP::MLC-4DD (green) and the junctional marker DLG-1::RFP (red) in a 1.5-fold embryo. Note the occurrence of thick myosin cables at positions distinct from cell-cell junctions. For all panels, anterior is to the left and dorsal is up. S, seam cells; D, dorsal cells. Scale bars: 5 μm.

2002; Sun et al., 2001). We confirmed that the distribution of this probe (referred to below as ABD::GFP) coincides with phalloidin staining (see Fig. S1A-C in the supplementary material). The ABD::GFP fluorescence was initially detected along the lateral membranes of epidermal cells before dorsal intercalation, and then was restricted apically (see Fig. S1F,G in the supplementary material).

Starting at the 1.2-fold stage, MFs formed a complex meshwork in all epidermal cells (Fig. 1A-A″) that was highly dynamic. Indeed, time-lapse experiments showed rapid polymerization and shortening events (between 3 μm and 10 μm per second, n=5 cables); although we are observing an actin-binding reporter rather than actin itself, these measures are quite comparable to observations performed in cell culture using mDIA1 (DIAP1 – Mouse Genome Informatics) (Higashida et al., 2004). Subsequently, in seam cells, MFs remained rather short and fuzzy throughout elongation (Fig. 1A-D,A′-D′). By contrast, in dorsal and ventral epidermal cells (DV cells), MFs progressively formed evenly spaced parallel circumferential bundles (CFBs) (Fig. 1B-B″), particularly after the 2-fold stage when muscle contractions begin (Fig. 1C-C″). Some apparent discontinuities could be reproducibly observed in DV cells at the 2-fold stage (Fig. 1C″, arrowhead; see Fig. S1H-I′ in the supplementary material), but were disappearing after the 3- to 3.5-fold stage (Fig. 1D-D″). Their position was consistent with that of muscle anchoring structures (fibrous organelles), indicating that CFBs might run from adherent junctions to fibrous organelles rather than from one seam border to the other. The number of CFBs was constant between the 2- and 3.5-fold stages in DV cells, with ~351±18 CFBs per embryo (n=15 embryos), in agreement with previous estimates (Costa et al., 1997). At the pretzel stage, actin bundles disassembled (data not shown).

Myosin II organization during elongation

Remodeling of actin MFs is often driven by non-muscle myosin II (Conti and Adelstein, 2008). To determine whether this is the case during *C. elegans* embryonic elongation, we examined the precise organization of myosin II. We generated a GFP N-terminal translational fusion for MLC-4/RMLC (referred to here as GFP::MLC-4WT), which could rescue the embryonic lethality and elongation defects of a strong *mlc-4* mutant and displayed a filamentous pattern (see Fig. S2A,C in the supplementary material; Fig. 2B,C). As embryos move vigorously beyond the 1.8-fold stage, we anaesthetized embryos by oxygen deprivation to precisely describe the pattern (see Materials and methods). However, this treatment induced the rapid disappearance of filaments (see Fig. S2B in the supplementary material).

As part of our efforts to dissect the molecular regulation of MLC-4 (see below), we noticed that a phosphomimetic form of MLC-4, in which residues T17 and S18 were changed into aspartate (GFP::MLC-4DD), formed a stable filamentous-like pattern even in the absence of oxygen (Fig. 1E-H). We therefore used this modified form to examine MLC-4 distribution, as the GFP::MLC-4DD reporter showed a pattern similar to the wild-type reporter (compare Fig. 1H with Fig. S2C in the supplementary material). We observed that MLC-4 is zygotically first detected during dorsal intercalation (data not shown). The expression level of GFP::MLC-4DD (Fig. 1E-H) was higher in seam cells than in DV cells at all stages. In seam cells, starting at the 1.2-fold stage, GFP::MLC-4DD formed aggregates (Fig. 1E-E″) that were not systematically associated with cell junctions (Fig. 1J). These aggregates evolved into a meshwork (Fig. 1F′-H′), which was reminiscent of the actomyosin meshwork that establishes embryonic polarity in *C. elegans* zygotes (Munro et

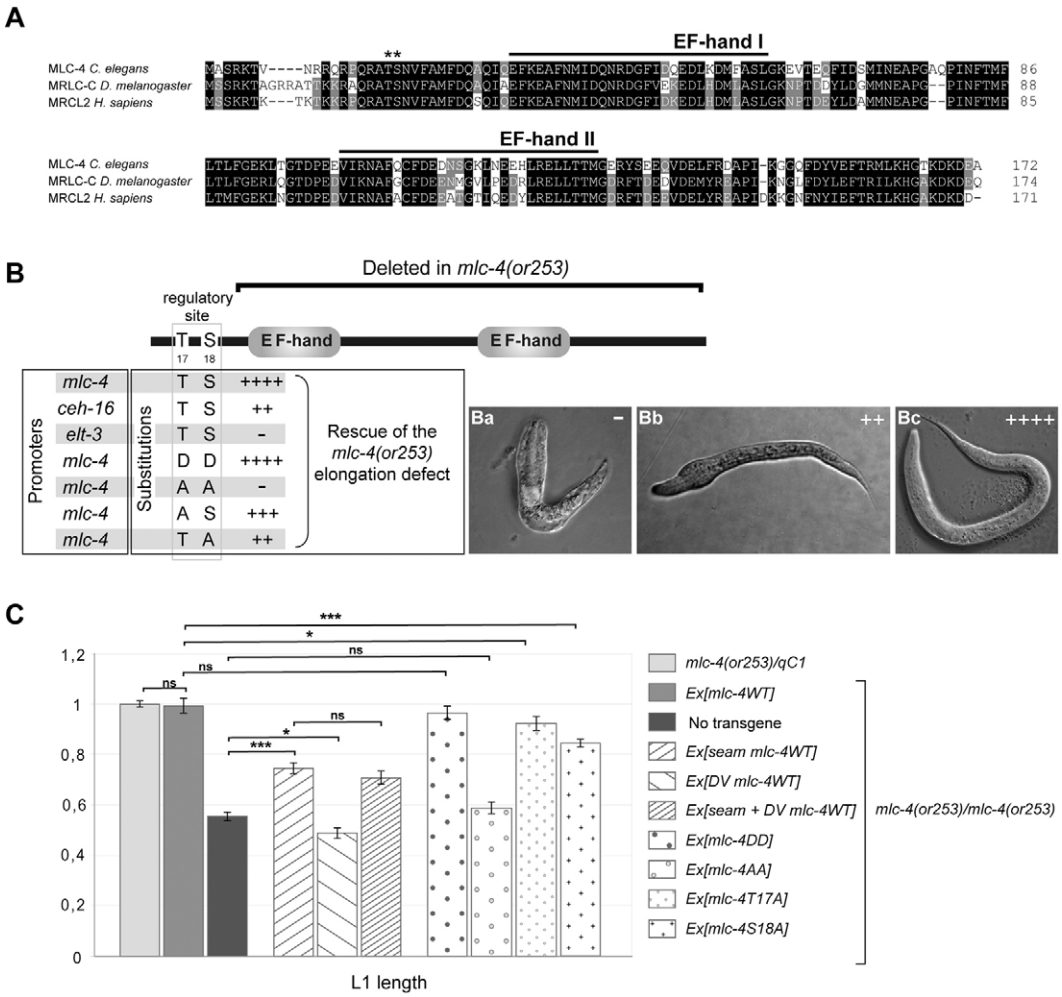

Fig. 2. Regulation of MLC-4 activity. (**A**) Alignment of MLC-4 with *Drosophila* and human orthologs. Asterisks, putative regulatory residues; black bars, EF-hand domains. (**B**) Summary of rescue experiments. + and –, rescue level of the *mlc-4(or253)* elongation defects: ++++, >95% wild-type length; +++, >85%; ++, >75%; +, >65%; –, <55%. Note that *mlc-4(or253)* homozygotes represent 59% of the wild-type length. (**Ba**) Non-rescued *mlc-4(or253)* mutant with strong elongation defect; (**Bb**) intermediate rescue observed for *mlc-4S18A* construct; (**Bc**) fully rescued L1 larva carrying the *mlc-4WT* construct. (**C**) Bar graph showing the length of freshly hatched transgenic *mlc-4(or253)* homozygotes normalized to that of wild-type *mlc-4(or253)/qC1* L1 larvae. Error bars indicate s.e.m. ***, $P<0.0001$; *, $P<0.05$; ns, not significant. For the different constructs, total numbers examined are the following: *mlc-4WT*, $n=27$; *seam mlc-4WT*, $n=17$; *DV mlc-4WT, n=20*; *seam + DV mlc-4WT*, $n=36$; *mlc-4DD*, $n=29$; *mlc-4AA*, $n=24$; *mlc-4T17A*, $n=20$; *mlc-4S18A*, $n=15$.

al., 2004). By contrast, in DV cells, the GFP::MLC-4DD fusion protein formed puncta (Fig. 1E″) that progressively became aligned and denser, until they formed filaments (Fig. 1F″-H″) overlapping actin (Fig. 1I). GFP::MLC-4 was also detected in adults (see Fig. S3 in the supplementary material). Together, the distinct patterns of MFs and myosin II in seam versus DV cells argue that both cell types should play different roles during elongation.

MLC-4 function is required in the seam cells

To determine whether the high MLC-4 expression in seam cells is physiologically relevant, we performed tissue-specific rescue experiments by expressing the *GFP::mlc-4WT* construct either in DV cells using the *elt-3* promoter (Gilleard et al., 1999) or in seam cells using the *ceh-16* promoter (Cassata et al., 2005) (see Fig. S4 in the supplementary material). GFP::MLC-4WT expression in DV cells could not rescue the elongation defects of *mlc-4(or253)* mutants, despite having a normal localization, and was even reducing the size of *mlc-4* larvae for two out of three lines (Fig. 2B,C). By contrast, GFP::MLC-4WT expression in seam cells could significantly rescue *mlc-4* mutants, suggesting that seam cells are the main epidermal cells driving elongation. This rescue was not improved by the addition of both *ceh-16*- and *elt-3*-driven transgenes (Fig. 2C), indicating that the most likely explanation for this partial rescue resides in the strength of the *ceh-16* promoter relative to that of *mlc-4*. Together, these results provide the first direct demonstration of the major role played by seam cells in driving elongation.

Regulation of MLC-4 by phosphorylation

Phosphorylation of two highly conserved RMLC residues controls stress fiber formation in cell culture and cytokinesis in *Drosophila* (Jordan and Karess, 1997; Watanabe et al., 2007). To test whether phosphorylation of the corresponding residues in MLC-4 (threonine 17 and serine 18, T17 and S18, respectively) (Fig. 2A) regulates myosin II activity in *C. elegans*, we introduced point mutations into the *GFP::mlc-4WT* transgene. We generated four variants that were introduced into the *mlc-4(or253)* mutant: a constitutive

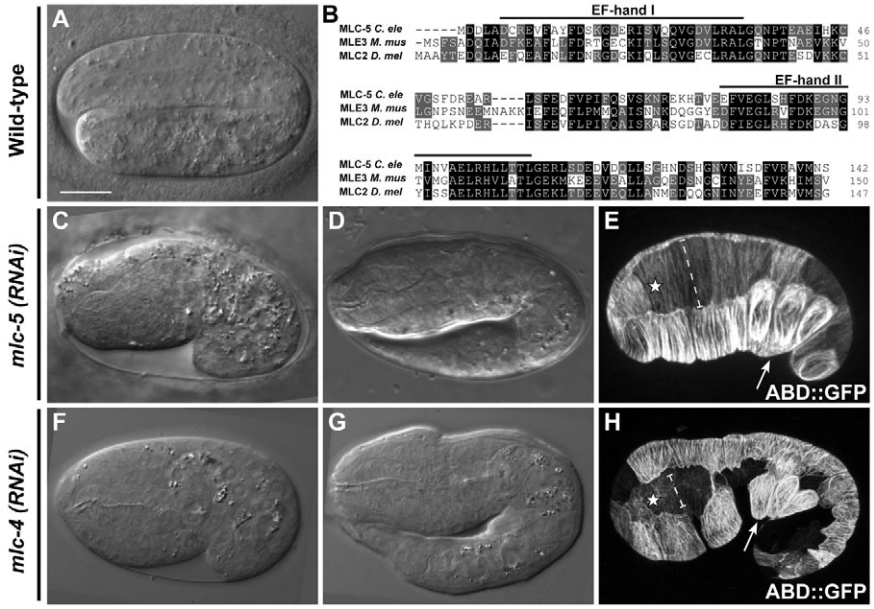

Fig. 3. MLC-5 is the *C. elegans* myosin II essential light chain. (**A**) DIC image of a wild-type 3-fold embryo. (**B**) Alignment of *mlc-5* with its murine and *Drosophila* orthologs. Black bars, EF-hand domains. (**C-H**) *mlc-5(RNAi)* (C-E) and *mlc-4*(*RNAi*) (F-H)-treated N2 embryos. The age of these embryos is comparable to that of the N2 embryo shown in A. (C,D,F,G) DIC pictures. The terminal phenotype depends on RNAi efficiency. (E,H) Confocal projections showing the actin network, which is distorted in three ventral cells (arrows). Seam cells (star) are enlarged (dashed line) compared with WT (Fig. 1D). Scale bar: 10 μm.

phosphomimetic form, *GFP::mlc-4(T17DS18D)* (referred to as *mlc-4DD*); a non-phosphorylatable form, *GFP::mlc-4(T17AS18A)* (referred to as *mlc-4AA*); and two mono-phosphorylatable forms, *GFP::mlc-4(S18A)* and *GFP::mlc-4(T17A)* (referred to as *mlc-4S18A* and *mlc-4T17A*, respectively) (Fig. 2B). Both GFP::MLC-4WT and GFP::MLC-4DD proteins could fully rescue the embryonic elongation defect of *mlc-4(or253)* mutants (Fig. 2B,C). Rescued L1 larvae further developed into sterile adults of normal length, presumably due to poor germline expression, as described previously (Shelton et al., 1999). Conversely, GFP::MLC-4AA could not rescue the *mlc-4(or253)* elongation defect (Fig. 2B,C), whereas constructs in which either S18 or T17 are replaced by alanine (*mlc-4S18A* or *mlc-4T17A*) partially rescued elongation of *mlc-4* mutants (Fig. 2B,C). Taken together, these experiments show that both T17 and S18 are required for MLC-4 function.

RNAi screens looking for regulators or components of the non-muscle myosin II

Our results highlight the importance of MLC-4 phosphorylation for its activity and actin association. Mains and co-workers predicted the existence of another kinase and possibly other myosin II regulators to account for the normal elongation of animals defective for both LET-502/ROCK and MEL-11/MYPT (Piekny et al., 2000; Wissmann et al., 1997). To identify such components, we designed two RNAi screens based on the following observations. Partial RNAi knockdown of MLC-4 (Fig. 3F) or of the myosin heavy chain NMY-2 in the *nmy-1* mutant background bypasses their early requirement for cytokinesis and leads to elongation arrest at the 1.2-fold stage (Piekny et al., 2003). We assumed that this phenotype reflects what should be observed when non-muscle myosin II is inactive, with essentially no maternal contribution specifically during elongation. Therefore we performed two RNAi screens in parallel, focusing in particular on genes whose knockdown causes arrest at the 1.2-fold stage.

In the first screen, we looked for severe elongation defects using the feeding RNAi library (Kamath and Ahringer, 2003). In the second screen, we targeted kinases known to regulate myosin II in other systems. As described below, the first screen led to the identification of the myosin II essential light chain, whereas the second identified kinases acting in parallel to LET-502/ROCK.

Identification of a new essential myosin light chain

Using a strain hypersensitive to RNAi for the first screen, we focused on genes previously shown to be essential for embryogenesis (Kamath and Ahringer, 2003), but eliminated genes predicted to be involved in general metabolism or transcription. Among the seven candidates retained (see Table S1 in the supplementary material), we characterized *T12D8.6*, the knockdown of which induced a strong elongation defect very similar to that observed in embryos lacking the two myosin heavy chains NMY-1 and NMY-2 (Piekny et al., 2003). We named *T12D8.6 mlc-5*, as its predicted translation product displays strong homology (45% and 55% identity over its EF-hand domains) (Fig. 3B) to vertebrate and *Drosophila* myosin essential light chains (Edwards et al., 1995; Robert et al., 1984) (see Fig. S5 in the supplementary material).

mlc-5 RNAi by injection in adults mainly induced embryonic elongation defects ranging from 1.2- to 2-fold arrest (Fig. 3C,D), as observed for *mlc-4* RNAi (Fig. 3F,G). Embryos failed to shorten circumferentially (compare dashed lines in Fig. 1D and Fig. 3E). Although the overall pattern of actin bundles was not dramatically affected after knocking down *mlc-5* (Fig. 3E) or *mlc-4* (Fig. 3H), it was partially distorted in ventral cells, making sometimes thicker bundles (Fig. 3E,H, arrow), indicating that myosin II only plays a minor role in organizing CFBs. This conclusion can only be tentative because such embryos must still contain some MLC-4 or MLC-5, as their complete absence arrests embryogenesis at the 1-cell stage (see Fig. S6E,G in the supplementary material) (Shelton et al., 1999).

The phenotype observed in MLC-5-depleted embryos suggests that MLC-5 could be part of the myosin II complex. To test this hypothesis, we generated an MLC-5 N-terminal GFP translational fusion (Fig. 4A). GFP::MLC-5 was first detected during dorsal intercalation (data not shown). It was then highly expressed in seam cells and to a lesser extent in DV cells (Fig. 4B), where it formed oxygen-sensitive parallel bundles starting at the 2-fold stage (Fig. 4C,D) overlapping with actin (Fig. 4E-G), like GFP::MLC-4. In *mlc-4* knockdown embryos, GFP::MLC-5 failed to form bundles and instead formed aggregates (Fig. 4H-J), as previously observed for NMY-1 in *mlc-4* mutant embryos (Piekny et al., 2003). Conversely, in *mlc-5* knockdown embryos, GFP::MLC-4 formed

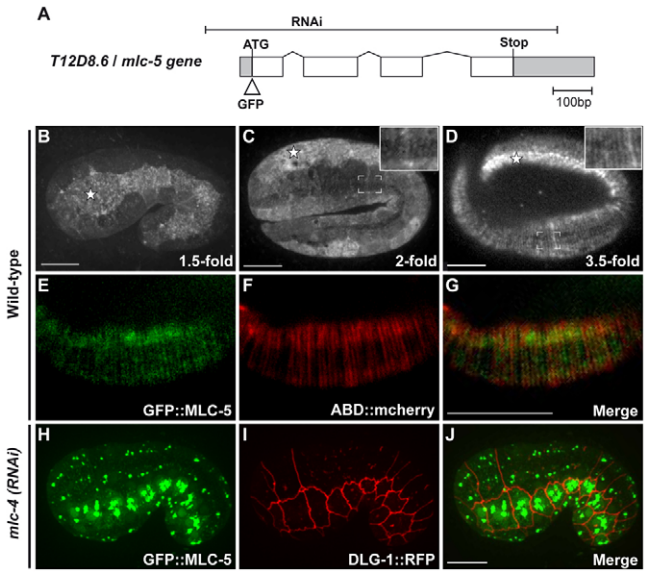

Fig. 4. MLC-5 localization in wild-type and *mlc-4(RNAi)* backgrounds. (**A**) Physical map of the *mlc-5* gene showing the GFP insertion site. Bracketed line indicates region targeted in RNAi experiments. (**B-D**) Spinning-disk confocal images of *GFP::mlc-5* transgenic embryos. MLC-5 expression is initially stronger in seam cells (star in B) and forms parallel bundles in DV cells starting at the 2-fold stage (insets in C,D). (**E-G**) Confocal projections of GFP::MLC-5 (E) and $ABD_{VAB\text{-}10}$::mCherry (actin; F), showing an overlap of both markers (G). (**H-J**) *mlc-4(RNAi)*-treated animals coexpressing GFP::MLC-5 (H) and the junctional marker DLG-1::RFP (I). (J) Merge; note the large aggregates in the middle of the seam cells and the smaller dots in the DV cells. Scale bars: 10 μm.

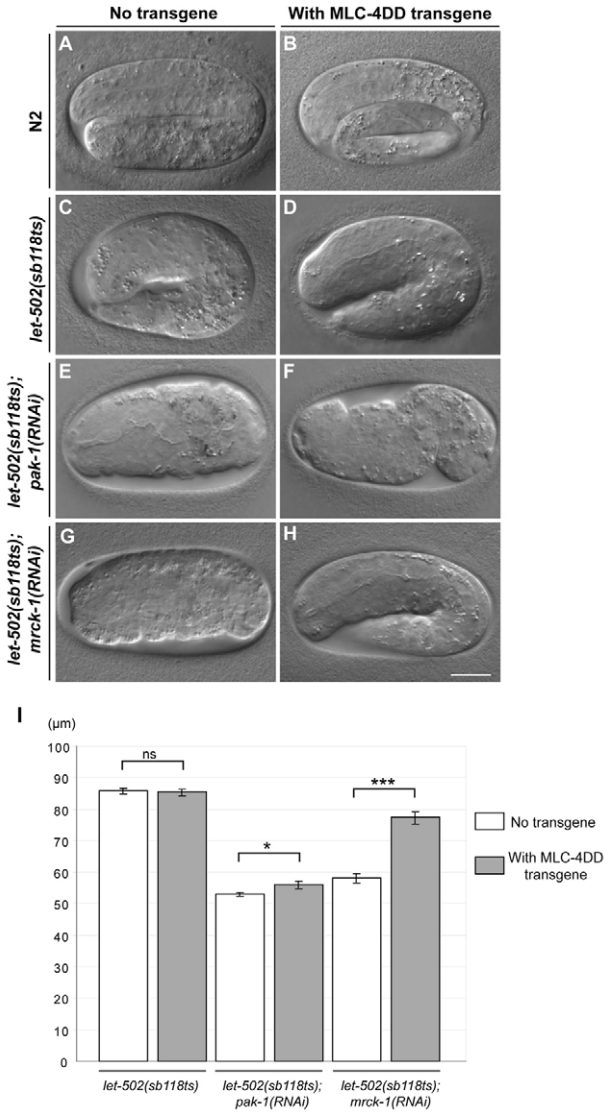

Fig. 5. *pak-1*, *mrck-1* and *let-502* act redundantly during elongation. (**A-H**) DIC images of wild-type (A,B), *let-502(sb118ts)* (C,D), *let-502(sb118ts);pak-1(RNAi)* (E,F) and *let-502(sb118ts);mrck-1(RNAi)* (G,H) embryos at the restrictive temperature of 25.5°C. Control (A,C,E,G) and transgenic (B,D,F,H) animals with the MLC-4DD construct. (**I**) Bar graph showing the length of *let-502(sb118ts)*, *let-502(sb118ts);pak-1(RNAi)* and *let-502(sb118ts);mrck-1(RNAi)* arrested embryos without (white bars) or with (gray bars) the MLC-4DD transgene. Error bars indicate s.e.m. ***, $P<0.0001$; *, $P<0.05$; ns, not significant. Scale bar: 10 μm.

small aggregates or was rather diffuse (data not shown), as observed for the GFP::MLC-4AA mutant form described above (see Fig. S2E in the supplementary material). To confirm that MLC-5 is part of the myosin II complex, we also observed the distribution of the myosin heavy chain NMY-2 after strong *mlc-5* RNAi induced by injection in L4 larvae. Because NMY-2 is highly expressed in early embryos, we looked at the first cell division, a process that requires myosin II activity (see Fig. S6 in the supplementary material). We observed that *mlc-5(RNAi)* induced a strong cytokinesis defect (see Fig. S6E,G in the supplementary material) and that NMY-2::GFP failed to form a contractile ring (see Fig. S6F,H in the supplementary material). Thus, MLC-5 plays a major role during early embryonic development, like NMY-2 (Guo and Kemphues, 1996) and MLC-4 (Shelton et al., 1999). Altogether, our results suggest that myosin II assembly and/or interaction with actin filaments require(s) the presence of both MLC-4 and MLC-5.

PAK and MRCK homologs act in parallel to LET-502/ROCK

As mentioned above, at least one additional kinase has been predicted to act in parallel to LET-502. We assumed that its inactivation in the *let-502* mutant background would lead to an early elongation arrest such as that observed when *mlc-5* or *mlc-4* are depleted. To identify this unknown kinase, we performed an enhancer RNAi screen in the thermosensitive *let-502(sb118ts)* mutant, targeting kinases known to activate the RMLC in other systems (see Table S2 in the supplementary material) (Batchelder et al., 2007; Matsumura, 2005). The *let-502(sb118ts)* single mutant shows a characteristic 2-fold stage arrest at 25.5°C (Fig. 5C) (Diogon et al., 2007). Among the ten kinases tested (see Table S2 in the supplementary material), two of them aggravated the elongation phenotype of *let-502(sb118ts)* mutants, causing a 1.2-fold stage arrest (Fig. 5E,G; see Fig. S7 in the supplementary material) but did not display any elongation phenotype in control animals (not shown). These two kinases are the p21-activated kinase homolog PAK-1 and the myotonic dystrophy kinase-related cdc42-binding kinase homolog, MRCK-1 (Fig. 7B).

To define the cause of this severe elongation defect, we first characterized the actin cytoskeleton in double mutants. As in *mlc-4* or *mlc-5* knockdown embryos, there were only minor MF organization defects in single *let-502(sb118ts)* mutants and *let-*

A

line #	Parental Genotype (Homozygote)				Phenotype at 25.5°C		
	let-502	*mel-11*	*pak-1*	*mrck-1*	Terminal Phenotype	Lethality %	n
1	*sb118*	+	+	+	2-fold	100	371
2	+	*it26*	+	+	Rupture	100	342
3	+	+	*ok448*	+	L1 arrest (83%) Pre-el Emb(6%)	89	1042
4	+	+	+	*ok586*	L1 arrest (53%) Pre-el Emb (47%)	100	452
5	*sb118*	*it26*	+	+	Rupture (4%) 1.2-2-fold arrest (37%) L1 arrest (41%)	83	293
6	*sb118*	+	*ok448*	+	1.2-fold	100	258
7	*sb118*	+	+	*ok586*	Pre-el Emb	100	104
8	+	*it26*	*ok448*	+	Rupture	100	371
9	*sb118*	*it26*	*ok448*	+	1.2-fold	100	381
10	+	+	+	RNAi	L1 arrest (5%) Pre-el Emb (5%)	10	408
11	*sb118*	+	+	RNAi	1.2-fold	100	315
12	+	*it26*	+	RNAi	Rupture	100	219
13	+	+	*ok448*	RNAi	L1 arrest (84%) Pre-el Emb (6%)	90	630
14	*sb118*	*it26*	+	RNAi	Rupture (5%) 1.2-2-fold arrest (51%) L1 arrest (21%)	78	423
15	*sb118*	+	*ok448*	RNAi	1.2-fold	100	211
16	+	*it26*	*ok448*	RNAi	Rupture	100	317
17	*sb118*	*it26*	*ok448*	RNAi	1.2-fold	100	134

B

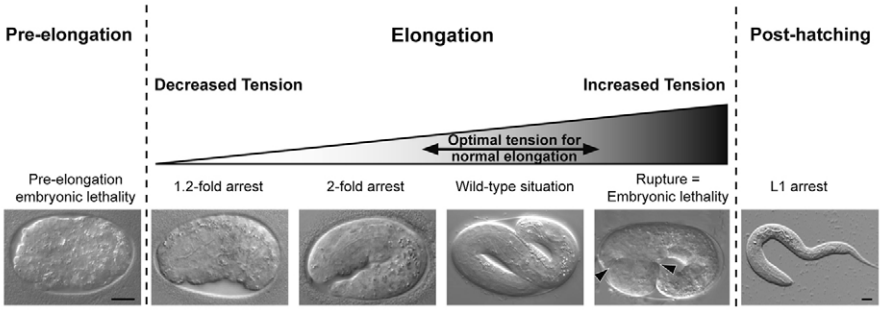

Fig. 6. Genetic interactions between *pak-1*, *mrck-1*, *let-502* and *mel-11*. (**A**) Table summarizing the genetic interactions between *pak-1*, *mrck-1*, *let-502* and *mel-11*. *n*, number of embryos counted to assess embryonic lethality; Pre-el Emb, Pre-elongation embryonic lethality. Note that *mel-11(it26);mrck-1(ok586)* mutants ruptured like *mel-11(it26);mrck-1(RNAi)* embryos. (**B**) Diagram and DIC images illustrating the main phenotypic classes, along with the inferred tensional defect. In the *mel-11(it26)* rupturing embryo (fifth from left), arrowheads indicate site of rupture. Scale bars: 10 μm.

502;pak-1 and *let-502;mrck-1* double mutants at the restrictive temperature (see Fig. S8 in the supplementary material), indicating that their elongation defect was not due to actin disorganization.

Using a functional assay, we then tested whether either kinase might be involved in MLC-4 phosphorylation. We examined whether the phosphomimetic MLC-4DD form described above could rescue the elongation defects of *let-502*, *let-502;pak-1(RNAi)* and *let-502;mrck-1(RNAi)* embryos. Indeed, in *Drosophila*, a phosphomimetic form of Sqh/RMLC allows 4% hemizygous *rok* (*Drosophila ROCK*) mutant survival until adulthood (Winter et al., 2001). We found that the *mlc-4DD* transgene could not rescue the elongation defects of *let-502(sb118ts)* (Fig. 5D,I) and poorly rescued the *let-502(sb118ts);pak-1(RNAi)* mutant elongation defects (Fig. 5F,I). These observations do not exclude the possibility that LET-502 and PAK-1 could phosphorylate MLC-4 (see Discussion). By contrast, the *mlc-4DD* transgene enabled *let-502(sb118ts);mrck-1(RNAi)* embryos to elongate until the 2-fold stage (Fig. 5H,I), indicating that a constitutively active form of myosin II can bypass the requirement for MRCK-1 kinase during elongation.

We observed a normal GFP::MLC-4WT pattern in *let-502(sb118ts);mrck-1(RNAi)* and *let-502(sb118ts);pak-1(ok448)* embryos (data not shown; see below for a description of the *pak-1(ok448)* allele), rather than the fuzzy pattern observed for MLC-4AA. This result might stem from the fact that neither *let-502(sb118ts)* nor RNAi against *mrck-1* are complete knockouts.

Genetic interactions between *let-502*, *mel-11*, *pak-1* and *mrck-1*

To further define the respective contribution of LET-502/ROCK, PAK-1 and MRCK-1 to embryonic elongation, we performed a genetic analysis. Specifically, we created all double and triple

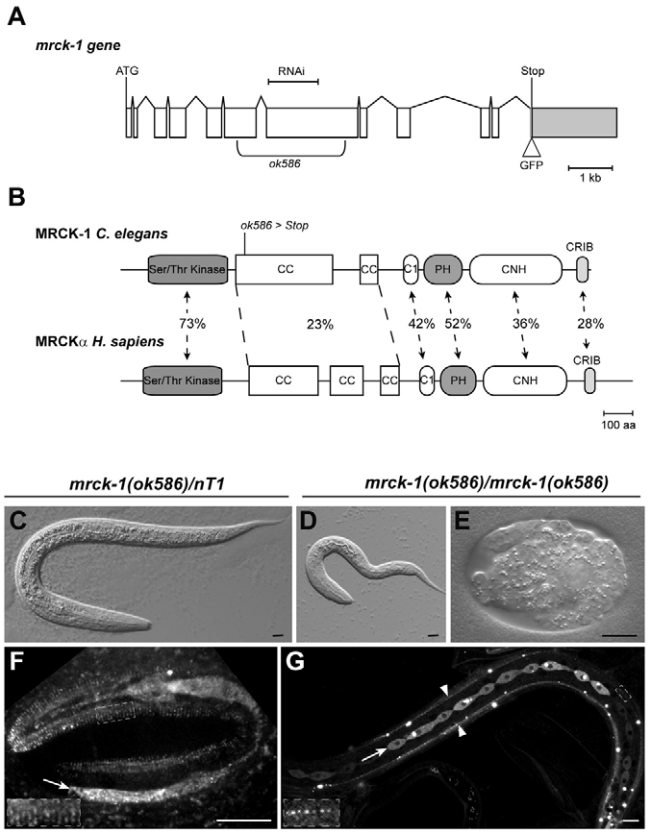

Fig. 7. MRCK-1 forms parallel bundles in the epidermis and is enriched in the seam cells. (**A**) Physical map of the *mrck-1* gene showing the fragment deleted in *mrck-1(ok586)* and the position of the GFP insertion. Bracketed line indicates region targeted in RNAi experiments. (**B**) Physical map of the MRCK-1 protein and its human ortholog, MRCKα. Ser/Thr kinase, kinase domain; CC, coiled-coils domain; C1, protein kinase C conserved region 1; PH, Pleckstrin homology domain; CNH, Citron homology domain; CRIB, Cdc42/Rac interactive binding region (SMART predictions). Numbers indicate percentage of identity between *C. elegans* and human domains. (**C-E**) DIC images of L1 larvae (C,D) or an arrested embryo (E) laid by heterozygous *mrck-1(ok586)/nT1* (C) and homozygous *mrck-1(ok586)* (D,E) mothers. (**F**,**G**) MRCK-1::GFP localization in a 3-fold embryo (F) or in an L4 larva (G). Arrows indicate seam cells. Arrowheads in G indicate the dorsal and ventral nerve cords. Inset in F shows the bundle pattern, inset in G shows sublateral presumptive synapses. Scale bars: 10 μm.

mutants for *let-502*, *pak-1*, *mrck-1* and the myosin phosphatase regulatory chain *mel-11*, to order them relative to each other in a genetic pathway.

To perform this analysis, we used a presumptive *mel-11* null allele, *mel-11(it26)*, which causes mutant embryos to rupture when they reach the 1.7-fold stage (Wissmann et al., 1999) (Fig. 6B). First, we used a *pak-1* deletion allele, *pak-1(ok448)*, which removes the kinase domain (a second allele, *tm403*, with a deletion in the CRIB domain confirmed most results). The *pak-1(ok448)* mutant induced L1 larval lethality at 25.5°C (Fig. 6A, line 3; Fig. 6B), and blocked elongation at the 1.2-fold stage when combined with *let-502(sb118ts)*, as observed after *pak-1(RNAi)* in the *let-502(sb118ts)* background (Fig. 6A, line 6; Fig. 6B). Second, we used a presumptive *mrck-1* null allele, *mrck-1(ok586)*, which removes the central part of the gene and causes a frameshift (Fig. 7A,B). Homozygous *mrck-1(ok586)* mutants can grow to adulthood, but subsequently give rise to progeny that arrest at the L1 stage (Fig. 7C,D) or during embryogenesis before elongation (Fig. 6B; Fig. 7E), indicating a maternal effect lethality. The *let-502(sb118ts);mrck-1(ok586)* double mutant displayed penetrant maternal-effect pre-morphogenesis defects, which we did not characterize further (Fig. 6A, line 7). This indicates that both genes are also redundant during early embryogenesis. Therefore, in further tests involving *mrck-1*, to circumvent the early requirement for MRCK-1, we used RNAi in adults, which avoids depletion of the maternal pool of *mrck-1* mRNA and preferentially affects the elongation stage.

When combined with *pak-1(ok448)* or *mrck-1(RNAi)*, the *mel-11(it26)* allele induced embryos to rupture, as observed in *mel-11* mutants alone (Fig. 6A, lines 8 and 12), indicating that *pak-1* and *mrck-1* act upstream of or in parallel to *mel-11*. Triple *let-502;mel-11;pak-1* mutants arrested at the 1.2-fold stage, like *let-502;pak-1* double mutants (Fig. 6A, lines 6 and 9). Hence, introducing *pak-1* cancels cosuppression by *let-502* and *mel-11*. By contrast, ~20% of triple *let-502;mel-11;mrck-1(RNAi)* mutants could reach adulthood, which is comparable to the proportion of *let-502;mel-11* double mutants surviving (Fig. 6A, lines 5 and 14). It confirms that MRCK-1 acts upstream of the *let-502/mel-11* pathway, and hence does not directly phosphorylate MLC-4. In the quadruple *let-502;mel-11;mrck-1(RNAi);pak-1* combination, all embryos failed to elongate (Fig. 6A, line 17). Thus, the *let-502;mel-11;mrck-1(RNAi)* embryos that elongated probably did so because PAK-1 could substitute for LET-502 and MRCK-1 in activating MLC-4.

MRCK-1 forms parallel bundles in the epidermis and is enriched in the seam cells

In order to describe further the role of MRCK-1 during elongation, we developed a C-terminal GFP translational fusion, MRCK-1::GFP (Fig. 7A). The construct was able to fully rescue the *mrck-1(ok586)* homozygous mutant. We observed that MRCK-1 is enriched in the seam cells, and forms parallel punctate bundles in the DV cells (Fig. 7F) very similar to those of GFP::MLC-4, but seemed to be excluded from junctions. The expression in seam cells persisted until adulthood (Fig. 7G). Furthermore MRCK-1::GFP was strongly expressed in the pharynx throughout development (not shown) and in the sublateral nerve cords (Fig. 7G), presumably at the level of synapses (Fig. 7G, inset). The presence of MRCK-1 in the nervous system might explain the L1 arrest. Altogether, MRCK-1 localization is consistent with the idea that it is involved in myosin II activation.

DISCUSSION

Non-muscle myosin II is thought to mediate most morphogenetic events involving epithelial cells. However, the mechanisms controlling its assembly and activity in vivo remain unclear. Here we provide an in-depth analysis of both of these aspects during *C. elegans* embryonic elongation, a process that involves junction remodeling and partial apical constriction (for a review, see Quintin et al., 2008).

New GFP probes to visualize the actomyosin cytoskeleton

Part of our work has relied on the introduction of novel GFP probes for live imaging of the actomyosin cytoskeleton. Instead of GFP::actin reporters, which we found to induce embryonic lethality and abnormally thick actin bundles (F.L., unpublished), we relied on the acting-binding domain of the spectraplakin VAB-10 (Bosher et al., 2003), which was expressed specifically in the epidermis. This probe faithfully recapitulates the distribution of actin as visualized

by phalloidin staining, and has already been successfully used by other labs (Lockwood et al., 2008; Patel et al., 2008). Other researchers have used the Moesin actin-binding domain for the same purpose (Edwards et al., 1997; Motegi and Sugimoto, 2006), a tool that is becoming very popular in the fly community.

Similarly, we generated a N-terminal GFP::MLC-4/RMLC fusion, which revealed a complex meshwork in the lateral seam cells and thin filaments in the dorsal and ventral epidermal cells. Although these structures had not been observed with a C-terminal GFP fusion (Shelton et al., 1999), we believe they reflect the bona fide position and organization of myosin II, because our novel GFP::MLC-5 construct revealed a similar pattern. Moreover, antibodies against the myosin heavy chain NMY-1 suggest a similar distribution (Piekny et al., 2003). Last, consistent with actin and myosin forming a common higher order complex, we found that the localization of both reporters mainly overlaps when they are combined.

Structure and assembly of the myosin II complex

The myosin II complex normally includes a heavy chain and two light chains. Our work strongly suggests that MLC-5 corresponds to the essential myosin light chain. First, sequence analysis shows that MLC-5 is more related to the human and *Drosophila* essential light chain than to any other EF-hand-containing proteins. Second, *mlc-5* knockdown induces cytokinesis defects and strong elongation defects, as reported when MLC-4/RMLC or both heavy chains are depleted (Piekny et al., 2003; Shelton et al., 1999). Third, the colocalization of GFP::MLC-5 with actin microfilaments depends on the presence of MLC-4 and, conversely, formation of the NMY-2-enriched contractile ring during cytokinesis depends on MLC-5.

Two lines of evidence indicate that MLC-4/RMLC phosphorylation favors its assembly into the myosin II complex. First, its distribution became rapidly diffuse in oxygen-deprived embryos, in which the ATP pool necessary for phosphorylation should rapidly dissipate. Second, the distribution of a non-phosphorylatable form of MLC-4 (MLC-4AA) was similarly diffuse in a homozygous *mlc-4* mutant. Conversely, a phosphomimetic form (MLC-4DD) retained its subcellular distribution even in the absence of oxygen. These results indicate that MLC-4 phosphorylation influences actin-myosin interactions. In vertebrate smooth muscles, RMLC phosphorylation appears to induce a conformational change in the heavy chain that destabilizes the interaction between its tail and the head-neck region, where the RMLC resides, to facilitate the formation of myosin filaments (for a review, see Ikebe, 2008). Likewise, in *Drosophila*, RMLC phosphorylation favors its recruitment to the cortex (Royou et al., 2002).

MLC-4 is preferentially required in the lateral cells

In contrast to most other well-characterized morphogenetic processes (Quintin et al., 2008), such as gastrulation and germband extension in *Drosophila* or *C. elegans* ventral enclosure, *C. elegans* embryonic elongation involves several types of epithelial cells (seam, ventral and dorsal cells). It had been predicted, based on their microtubule distribution and their enrichment for LET-502/ROCK and MLC-4, that seam cells should play a central role in elongation (Piekny et al., 2003; Priess and Hirsh, 1986; Shelton et al., 1999; Wissmann et al., 1999). However, this had not been formally established. Using seam-specific or DV-specific promoters to express MLC-4 in an *mlc-4* mutant, we indeed found that myosin II acts predominantly in the lateral seam cells. Our results are consistent with our previous finding showing that the RhoGAP RGA-2, which behaves as a negative regulator of myosin II, acts predominantly in DV cells (Diogon et al., 2007). Altogether, our data suggest that tension should be released in the DV cells, whereas it must be increased in seam cells, to achieve embryonic elongation. Along these lines, a physical modeling of the elongation process, taking into account the incompressibility of the embryo and the mechanical properties of the cytoskeleton, suggests that lateral cells are sufficient to induce the initial lengthening of the embryo (Ciarletta et al., 2009).

LET-502, PAK-1 and MRCK-1 play redundant roles during embryonic development

Biochemical analysis in vertebrates suggests that RMLC phosphorylation on serine 19 (S19) triggers myosin II motor activity, and that phosphorylation on threonine 18 (T18) together with S19 further increases its activity (Ikebe et al., 1986). Likewise, phosphorylation of *Drosophila* RMLC at the position equivalent to S19 is sufficient to induce myosin II activity (Jordan and Karess, 1997; Vereshchagina et al., 2004). Consistent with these data, we show that a phosphomimetic variant of MLC-4/RMLC (MLC-4DD) fully rescues the elongation defect of *mlc-4* mutants, whereas an unphosphorylatable form (MLC-4AA) fails to rescue the defect. Since the MLC-4T17A variant, which can still be phosphorylated on the adjacent serine (S18), rescued more significantly than the MLC-4S18A variant, we conclude that in *C. elegans* too, the serine plays a more crucial role in MLC-4/RMLC activation.

The kinase(s) that mediate RMLC phosphorylation during epithelial morphogenesis has not been systematically investigated before, although it has been assumed that ROCK should play a key role. We show that depletion of *let-502* with either *pak-1* or *mrck-1* leads to arrest at the 1.2-fold stage, which we consider as an absence of elongation. This phenotype is not due to dramatic actin disorganization, suggesting that these kinases play a role either in myosin II activation or in another process. We could not directly test whether the loss of these kinases affects MLC-4/RMLC phosphorylation using vertebrate phospho-RMLC antibodies due to technical problems. Although these antibodies have been successfully used in early *C. elegans* embryos (Jenkins et al., 2006; Lee et al., 2006; Piekny and Mains, 2002), we suspect that fixation protocols for immunohistochemistry modify the physiological properties of the embryo and mimic the oxygen-free conditions that affect MLC-4 distribution during elongation. Moreover, in early embryos, MLC-4 forms a local patch (cytokinetic ring, invaginating endoderm precursor, cortex of zygote), whereas we mainly need to see individual filaments during elongation.

To circumvent this technical limitation, we instead used a functional test. We demonstrated that a constitutively active form of myosin II can bypass the requirement for the MRCK-1 kinase in *let-502(sb118ts);mrck-1(RNAi)* embryos, suggesting that MRCK is a kinase responsible for myosin II activation, probably via an indirect process involving MEL-11 inactivation. Consistent with this idea, MRCK-1::GFP distribution is very similar to that of MLC-4. The same phosphomimetic form of MLC-4/RMLC could not rescue the elongation defects of *let-502(sb118ts)* and very poorly, yet significantly, rescued those of *let-502(sb118ts);pak-1(RNAi)* mutants. These observations do not exclude the possibility that LET-502/ROCK and PAK-1 could phosphorylate MLC-4 (see below), as occurs in vertebrates.

Our genetic epistasis data suggest that MRCK-1, but not PAK-1, acts upstream of MEL-11/MYPT in vivo. Indeed, we found that a significant proportion of *let-502;mel-11;mrck-1* triply defective embryos could normally elongate, but that removing *pak-1* in this background abrogates their elongation. In vertebrates, ROCK, PAK

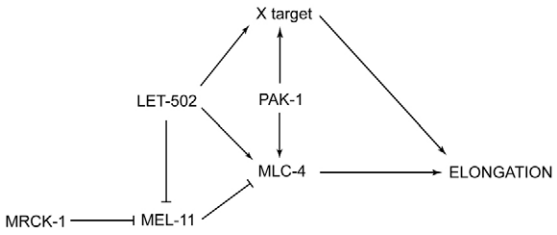

Fig. 8. Roles of LET-502, MEL-11, PAK-1 and MRCK-1 in embryonic elongation. See Discussion for details.

and MRCK can directly phosphorylate RMLC (Amano et al., 1996; Chew et al., 1998; Leung et al., 1998), as well as MYPT, to inhibit myosin phosphatase activity (Kimura et al., 1996; Takizawa et al., 2002; Tan et al., 2001), both of which induce myosin II activation. Integrating these biochemical data, we suggest that two parallel pathways can activate MLC-4/RMLC (Fig. 8): first, the redundant activities of LET-502/ROCK and MRCK phosphorylate, and thereby inactivate, MEL-11/MYPT; second, PAK-1, in parallel to LET-502/ROCK, can directly phosphorylate MLC-4/RMLC. Interestingly, our in vivo analysis is consistent with in vitro kinase assays with carcinoma cell extracts showing that the simultaneous inhibition of ROCK and MRCK dramatically decreases MYPT phosphorylation without affecting RMLC phosphorylation (Wilkinson et al., 2005). Wilkinson and co-workers proposed that ROCK and MRCK redundantly activate myosin II through the inhibition of myosin phosphatase, and that additional kinases phosphorylate RMLC, which the authors suggest are MLCK and ZIPK (Wilkinson et al., 2005). The closest *C. elegans* MLCK and ZIPK homologs (ZC373.4 and DAPK-1, respectively) do not act in parallel to *let-502* (see Table S2 in the supplementary material). Therefore, in addition to LET-502/ROCK, PAK-1 appears to be the best candidate kinase responsible for MLC-4/RMLC phosphorylation in the process of embryonic elongation. Although this is the simplest model, we cannot exclude the possibility that a fourth kinase distinct from PAK-1 phosphorylates MLC-4/RMLC to substitute for LET-502/ROCK and MRCK-1 when they are both absent.

Although we propose that LET-502/ROCK, PAK-1 and MRCK-1 directly and indirectly activate MLC-4/RMLC, their respective contributions are probably different. Indeed, the elongation phenotype of *let-502* single and *let-502;mrck-1* double mutants suggests that the resulting increase in MEL-11/MYPT activity is not compensated by the kinase activity of PAK-1. It argues that the ability of PAK-1 to phosphorylate MLC-4/RMLC is low compared with the ability of MEL-11/MYPT to dephosphorylate it.

Two genetic observations argue that PAK-1 and LET-502/ROCK activate a second process through phosphorylation, which occurs before or independently of myosin-II-based microfilament shortening (Fig. 8). First, as already recalled, the phosphomimetic form of MLC-4 could not rescue the *let-502;pak-1* double mutant. Second, a *pak-1* null allele prevented the mutual suppression observed between *let-502* and *mel-11*. What could this other process be that is regulated by LET-502/ROCK, PAK-1 and their targets? The elongation phenotype of *let-502;pak-1* is more similar to that observed when actin dynamics is pharmacologically inhibited than when microtubule dynamics is inhibited (Priess and Hirsh, 1986). The process could thus be actin based, even though we did not detect major actin defects, which is probably due to a lack of resolution and/or proper reagents.

The simplest hypothesis is that LET-502 and PAK-1 share a common target, besides MLC-4, that would be important for elongation. In vertebrates, ROCK and PAK phosphorylate common targets, such as intermediate filaments (IFs) or ERM (ezrin, radixin and moesin) proteins, promoting their reorganization (Goto et al., 1998; Goto et al., 2002) or ability to bind actin (Kissil et al., 2002; Matsui et al., 1998), respectively. However, *C. elegans* IF and ERM homologs are unlikely to be the relevant LET-502 and PAK-1 targets, as mutations affecting epidermal IFs or the unique ERM homolog, ERM-1, have either a less severe elongation phenotype or no elongation phenotype at all (Van Furden et al., 2004; Woo et al., 2004). Alternatively, one can imagine that LET-502 and PAK-1 phosphorylate two distinct targets that have redundant roles during elongation. For instance, human PAK1 can also phosphorylate filamin and a subunit of the Arp2/3 complex (for a review, see Arias-Romero and Chernoff, 2008). Therefore, changes in the actin network at the level of the cortex might facilitate its visco-elastic properties and allow junction remodeling. Alternatively, cortical myosin II might regulate actin network visco-elasticity, as observed for instance during cytokinesis (Girard et al., 2004). Future investigations should attempt to clarify these issues and allow the identification of target X.

To summarize, our study addresses for the first time in vivo the role of the three kinases LET-502/ROCK, PAK-1 and MRCK-1 in myosin II activation in a complex system involving different cell types. We show that these kinases have redundant roles during elongation of the *C. elegans* embryo, opening perspectives in the understanding of how myosin II regulation can promote complex morphogenetic processes.

Acknowledgements
We are grateful to the IGBMC Imaging Center for making available their new confocal microscopes, and particularly thank Marc Koch, Didier Hentsch and Jean-Luc Vonesch for constant support and advice. We thank Erik Jorgensen for the pCFJ90 plasmid, Edwin Munro for the NMY-2::GFP strain, the National Bioresource Project, the *C. elegans* Gene Knockout Consortium and the CGC for strains. F.W. was supported by fellowships from the Ministère de la Recherche and the Fondation pour la Recherche Médicale. This work was supported by grants from the European Union (FP6-STREP program), the ARC, the AFM, the ANR and from institutional funds from the CNRS and INSERM. This article is dedicated to the memory of Satis Sookhareea.

Supplementary material
Supplementary material for this article is available at
http://dev.biologists.org/cgi/content/full/136/18/3109/DC1

References
Amano, M., Ito, M., Kimura, K., Fukata, Y., Chihara, K., Nakano, T., Matsuura, Y. and Kaibuchi, K. (1996). Phosphorylation and activation of myosin by Rho-associated kinase (Rho-kinase). *J. Biol. Chem.* **271**, 20246-20249.
Arias-Romero, L. E. and Chernoff, J. (2008). A tale of two Paks. *Biol. Cell* **100**, 97-108.
Batchelder, E. L., Thomas-Virnig, C. L., Hardin, J. D. and White, J. G. (2007). Cytokinesis is not controlled by calmodulin or myosin light chain kinase in the *Caenorhabditis elegans* early embryo. *FEBS Lett.* **581**, 4337-4341.
Bosher, J. M., Hahn, B. S., Legouis, R., Sookhareea, S., Weimer, R. M., Gansmuller, A., Chisholm, A. D., Rose, A. M., Bessereau, J. L. and Labouesse, M. (2003). The *Caenorhabditis elegans vab-10* spectraplakin isoforms protect the epidermis against internal and external forces. *J. Cell Biol.* **161**, 757-768.
Brenner, S. (1974). The genetics of *Caenorhabditis elegans*. *Genetics* **77**, 71-94.
Cassata, G., Shemer, G., Morandi, P., Donhauser, R., Podbilewicz, B. and Baumeister, R. (2005). *ceh-16/engrailed* patterns the embryonic epidermis of *Caenorhabditis elegans*. *Development* **132**, 739-749.
Chew, T. L., Masaracchia, R. A., Goeckeler, Z. M. and Wysolmerski, R. B. (1998). Phosphorylation of non-muscle myosin II regulatory light chain by p21-activated kinase (gamma-PAK). *J. Muscle Res. Cell Motil.* **19**, 839-854.
Chisholm, A. D. and Hardin, J. (2005). Epidermal morphogenesis. In *WormBook* (ed. The *C. elegans* Research Community), doi:10.1895/wormbook.1.35.1, http://www.wormbook.org.

Ciarletta, P. M., B. A. and Labouesse, M. (2009). Continuum model of epithelial morphogenesis during *C. elegans* embryonic elongation. *Philos. Trans. R. Soc. Lond. A* (in press).
Conti, M. A. and Adelstein, R. S. (2008). Nonmuscle myosin II moves in new directions. *J. Cell Sci.* **121**, 11-18.
Costa, M., Draper, B. and Priess, J. (1997). The role of actin filaments in patterning the *Caenorhabditis elegans* cuticle. *Dev. Biol.* **184**, 373-384.
Diogon, M., Wissler, F., Quintin, S., Nagamatsu, Y., Sookhareea, S., Landmann, F., Hutter, H., Vitale, N. and Labouesse, M. (2007). The RhoGAP RGA-2 and LET-502/ROCK achieve a balance of actomyosin-dependent forces in *C. elegans* epidermis to control morphogenesis. *Development* **134**, 2469-2479.
Edwards, K. A., Chang, X. J. and Kiehart, D. P. (1995). Essential light chain of *Drosophila* nonmuscle myosin II. *J. Muscle Res. Cell Motil.* **16**, 491-498.
Edwards, K. A., Demsky, M., Montague, R. A., Weymouth, N. and Kiehart, D. P. (1997). GFP-moesin illuminates actin cytoskeleton dynamics in living tissue and demonstrates cell shape changes during morphogenesis in *Drosophila*. *Dev. Biol.* **191**, 103-117.
Gilleard, J. S., Shafi, Y., Barry, J. D. and McGhee, J. D. (1999). ELT-3: a *Caenorhabditis elegans* GATA factor expressed in the embryonic epidermis during morphogenesis. *Dev. Biol.* **208**, 265-280.
Girard, K. D., Chaney, C., Delannoy, M., Kuo, S. C. and Robinson, D. N. (2004). Dynacortin contributes to cortical viscoelasticity and helps define the shape changes of cytokinesis. *EMBO J.* **23**, 1536-1546.
Goto, H., Kosako, H., Tanabe, K., Yanagida, M., Sakurai, M., Amano, M., Kaibuchi, K. and Inagaki, M. (1998). Phosphorylation of vimentin by Rho-associated kinase at a unique amino-terminal site that is specifically phosphorylated during cytokinesis. *J. Biol. Chem.* **273**, 11728-11736.
Goto, H., Tanabe, K., Manser, E., Lim, L., Yasui, Y. and Inagaki, M. (2002). Phosphorylation and reorganization of vimentin by p21-activated kinase (PAK). *Genes Cells* **7**, 91-97.
Guo, S. and Kemphues, K. J. (1996). A non-muscle myosin required for embryonic polarity in *Caenorhabditis elegans*. *Nature* **382**, 455-458.
Higashida, C., Miyoshi, T., Fujita, A., Oceguera-Yanez, F., Monypenny, J., Andou, Y., Narumiya, S. and Watanabe, N. (2004). Actin polymerization-driven molecular movement of mDia1 in living cells. *Science* **303**, 2007-2010.
Ikebe, M. (2008). Regulation of the function of mammalian myosin and its conformational change. *Biochem. Biophys. Res. Commun.* **369**, 157-164.
Ikebe, M., Hartshorne, D. J. and Elzinga, M. (1986). Identification, phosphorylation, and dephosphorylation of a second site for myosin light chain kinase on the 20,000-dalton light chain of smooth muscle myosin. *J. Biol. Chem.* **261**, 36-39.
Jenkins, N., Saam, J. R. and Mango, S. E. (2006). CYK-4/GAP provides a localized cue to initiate anteroposterior polarity upon fertilization. *Science* **313**, 1298-1301.
Jordan, P. and Karess, R. (1997). Myosin light chain-activating phosphorylation sites are required for oogenesis in *Drosophila*. *J. Cell Biol.* **139**, 1805-1819.
Kamath, R. and Ahringer, J. (2003). Genome-wide RNAi screening in *Caenorhabditis elegans*. *Methods* **30**, 313-321.
Kamath, R., Fraser, A., Dong, Y., Poulin, G., Durbin, R., Gotta, M., Kanapin, A., Le Bot, N., Moreno, S., Sohrmann, M. et al. (2003). Systematic functional analysis of the *Caenorhabditis elegans* genome using RNAi. *Nature* **421**, 231-237.
Kimura, K., Ito, M., Amano, M., Chihara, K., Fukata, Y., Nakafuku, M., Yamamori, B., Feng, J., Nakano, T., Okawa, K. et al. (1996). Regulation of myosin phosphatase by Rho and Rho-associated kinase (Rho-kinase). *Science* **273**, 245-248.
Kissil, J. L., Johnson, K. C., Eckman, M. S. and Jacks, T. (2002). Merlin phosphorylation by p21-activated kinase 2 and effects of phosphorylation on merlin localization. *J. Biol. Chem.* **277**, 10394-10399.
Landmann, F., Quintin, S. and Labouesse, M. (2004). Multiple regulatory elements with spatially and temporally distinct activities control the expression of the epithelial differentiation gene *lin-26* in *C. elegans*. *Dev. Biol.* **265**, 478-490.
Lee, J. Y., Marston, D. J., Walston, T., Hardin, J., Halberstadt, A. and Goldstein, B. (2006). Wnt/Frizzled signaling controls *C. elegans* gastrulation by activating actomyosin contractility. *Curr. Biol.* **16**, 1986-1997.
Lee, S. and Kolodziej, P. A. (2002). Short Stop provides an essential link between F-actin and microtubules during axon extension. *Development* **129**, 1195-1204.
Leung, T., Chen, X. Q., Tan, I., Manser, E. and Lim, L. (1998). Myotonic dystrophy kinase-related Cdc42-binding kinase acts as a Cdc42 effector in promoting cytoskeletal reorganization. *Mol. Cell. Biol.* **18**, 130-140.
Lockwood, C., Zaidel-Bar, R. and Hardin, J. (2008). The *C. elegans* zonula occludens ortholog cooperates with the cadherin complex to recruit actin during morphogenesis. *Curr. Biol.* **18**, 1333-1337.
Matsui, T., Maeda, M., Doi, Y., Yonemura, S., Amano, M., Kaibuchi, K., Tsukita, S. and Tsukita, S. (1998). Rho-kinase phosphorylates COOH-terminal threonines of ezrin/radixin/moesin (ERM) proteins and regulates their head-to-tail association. *J. Cell Biol.* **140**, 647-657.
Matsumura, F. (2005). Regulation of myosin II during cytokinesis in higher eukaryotes. *Trends Cell Biol.* **15**, 371-377.
Motegi, F. and Sugimoto, A. (2006). Sequential functioning of the ECT-2 RhoGEF, RHO-1 and CDC-42 establishes cell polarity in *Caenorhabditis elegans* embryos. *Nat. Cell Biol.* **8**, 978-985.
Munro, E., Nance, J. and Priess, J. R. (2004). Cortical flows powered by asymmetrical contraction transport PAR proteins to establish and maintain anterior-posterior polarity in the early *C. elegans* embryo. *Dev. Cell* **7**, 413-424.
Patel, F. B., Bernadskaya, Y. Y., Chen, E., Jobanputra, A., Pooladi, Z., Freeman, K. L., Gally, C., Mohler, W. A. and Soto, M. C. (2008). The WAVE/SCAR complex promotes polarized cell movements and actin enrichment in epithelia during *C. elegans* embryogenesis. *Dev. Biol.* **324**, 297-309.
Piekny, A. J. and Mains, P. E. (2002). Rho-binding kinase (LET-502) and myosin phosphatase (MEL-11) regulate cytokinesis in the early *Caenorhabditis elegans* embryo. *J. Cell Sci.* **115**, 2271-2282.
Piekny, A. J., Wissmann, A. and Mains, P. E. (2000). Embryonic morphogenesis in *Caenorhabditis elegans* integrates the activity of LET-502 Rho-binding kinase, MEL-11 myosin phosphatase, DAF-2 insulin receptor and FEM-2 PP2c phosphatase. *Genetics* **156**, 1671-1689.
Piekny, A. J., Johnson, J. L., Cham, G. D. and Mains, P. E. (2003). The *Caenorhabditis elegans* nonmuscle myosin genes *nmy-1* and *nmy-2* function as redundant components of the *let-502*/Rho-binding kinase and *mel-11*/myosin phosphatase pathway during embryonic morphogenesis. *Development* **130**, 5695-5704.
Priess, J. R. and Hirsh, D. I. (1986). *Caenorhabditis elegans* morphogenesis: the role of the cytoskeleton in elongation of the embryo. *Dev. Biol.* **117**, 156-173.
Quintin, S., Gally, C. and Labouesse, M. (2008). Epithelial morphogenesis in embryos: asymmetries, motors and brakes. *Trends Genet.* **24**, 221-230.
Robert, B., Daubas, P., Akimenko, M. A., Cohen, A., Garner, I., Guenet, J. L. and Buckingham, M. (1984). A single locus in the mouse encodes both myosin light chains 1 and 3, a second locus corresponds to a related pseudogene. *Cell* **39**, 129-140.
Royou, A., Sullivan, W. and Karess, R. (2002). Cortical recruitment of nonmuscle myosin II in early syncytial *Drosophila* embryos: its role in nuclear axial expansion and its regulation by Cdc2 activity. *J. Cell Biol.* **158**, 127-137.
Shelton, C. A., Carter, J. C., Ellis, G. C. and Bowerman, B. (1999). The nonmuscle myosin regulatory light chain gene *mlc-4* is required for cytokinesis, anterior-posterior polarity, and body morphology during *Caenorhabditis elegans* embryogenesis. *J. Cell Biol.* **146**, 439-451.
Somlyo, A. P. and Somlyo, A. V. (2003). Ca^{2+} sensitivity of smooth muscle and nonmuscle myosin II: modulated by G proteins, kinases, and myosin phosphatase. *Physiol. Rev.* **83**, 1325-1358.
Sun, D., Leung, C. L. and Liem, R. K. (2001). Characterization of the microtubule binding domain of microtubule actin crosslinking factor (MACF): identification of a novel group of microtubule associated proteins. *J. Cell Sci.* **114**, 161-172.
Takizawa, N., Koga, Y. and Ikebe, M. (2002). Phosphorylation of CPI17 and myosin binding subunit of type 1 protein phosphatase by p21-activated kinase. *Biochem. Biophys. Res. Commun.* **297**, 773-778.
Tan, I., Ng, C. H., Lim, L. and Leung, T. (2001). Phosphorylation of a novel myosin binding subunit of protein phosphatase 1 reveals a conserved mechanism in the regulation of actin cytoskeleton. *J. Biol. Chem.* **276**, 21209-21216.
Van Furden, D., Johnson, K., Segbert, C. and Bossinger, O. (2004). The *C. elegans* ezrin-radixin-moesin protein ERM-1 is necessary for apical junction remodelling and tubulogenesis in the intestine. *Dev. Biol.* **272**, 262-276.
Vereshchagina, N., Bennett, D., Szoor, B., Kirchner, J., Gross, S., Vissi, E., White-Cooper, H. and Alphey, L. (2004). The essential role of PP1beta in *Drosophila* is to regulate nonmuscle myosin. *Mol. Biol. Cell* **15**, 4395-4405.
Watanabe, T., Hosoya, H. and Yonemura, S. (2007). Regulation of myosin II dynamics by phosphorylation and dephosphorylation of its light chain in epithelial cells. *Mol. Biol. Cell* **18**, 605-616.
Wilkinson, S., Paterson, H. F. and Marshall, C. J. (2005). Cdc42-MRCK and Rho-ROCK signalling cooperate in myosin phosphorylation and cell invasion. *Nat. Cell Biol.* **7**, 255-261.
Winter, C. G., Wang, B., Ballew, A., Royou, A., Karess, R., Axelrod, J. D. and Luo, L. (2001). *Drosophila* Rho-associated kinase (Drok) links Frizzled-mediated planar cell polarity signaling to the actin cytoskeleton. *Cell* **105**, 81-91.
Wissmann, A., Ingles, J., McGhee, J. D. and Mains, P. E. (1997). *Caenorhabditis elegans* LET-502 is related to Rho-binding kinases and human myotonic dystrophy kinase and interacts genetically with a homolog of the regulatory subunit of smooth muscle myosin phosphatase to affect cell shape. *Genes Dev.* **11**, 409-422.
Wissmann, A., Ingles, J. and Mains, P. E. (1999). The *Caenorhabditis elegans mel-11* myosin phosphatase regulatory subunit affects tissue contraction in the somatic gonad and the embryonic epidermis and genetically interacts with the Rac signaling pathway. *Dev. Biol.* **209**, 111-127.
Woo, W. M., Goncharov, A., Jin, Y. and Chisholm, A. D. (2004). Intermediate filaments are required for *C. elegans* epidermal elongation. *Dev. Biol.* **267**, 216-229.

Table S1. Genes and associated RNAi phenotypes for candidates obtained in the RNAi screen for elongation or cytoskeleton defects

Category	Transcript	Gene name	Function	Phenotype*	Penetrance†
Cytoskeleton associated	T12D8.6	*mlc-5*	Myosin essential light chain	No cytokinesis, arrest at 1.2-fold	100%
	Y66H1B.3	*filamin*	Cytoskeletal crosslinker	BMD, arrest before 2-fold, disorganised cytoskeleton	25%
	W07B3.2	*gei-4*	Regulator of intermediate filaments	BMD, arrest before 2-fold	20%
Trafficking	C56C10.3	*vps-32*	Protein sorting	BMD, arrest before 1.5-fold, defects in seam cell alignment	100%
	ZC518.2	*sec-24*	ER-to-Golgi transport	Arrest before 2-fold	60%
Unknown	F33H1.3			BMD, arrest before 2-fold	40%
	R08D7.2			BMD, arrest before 1.5-fold	20%

*Phenotype observed after RNAi feeding on *rrf-3(pk1426)* background.
†Percentage of embryos displaying the described phenotype.
BMD, body morphology defects.

Table S2. RNAi phenotype of potential myosin light chain kinases in a *let-502* mutant background

Genotype	Human ortholog	Elongation arrest at 25.5°C*	Penetrance†
N2		No	98%
let-502(sb118ts)		2-fold	98%
let-502(sb118ts);spk-1(RNAi)	SR-protein-specific kinase 1	2-fold	90%
slet-502(sb118ts);dapk-1(RNAi)	Death-associated protein kinase 1	2-fold	91%
let-502(sb118ts);aak-1(RNAi)	AMPK alpha-1 chain	2-fold	95%
let-502(sb118ts);aak-2(RNAi)	AMPK alpha-2 chain	2-fold	94%
let-502(sb118ts);gck-1(RNAi)	STE20-like kinase	2-fold	95%
let-502(sb118ts);gck-2(RNAi)	MEKKK 5	2-fold	92%
let-502(sb118ts);mig-15(RNAi)	MEKKK 4	2-fold	95%
let-502(sb118ts);ZC373.4(RNAi)	MLCK	2-fold	83%
let-502(sb118ts);mrck-1(RNAi)	MRCK	1.2-fold	90%
let-502(sb118ts);pak-1(RNAi)	p21-activated kinase 1	1.2-fold	98%

*N2 and *let-502(sb118ts)* young adults were injected with double-stranded RNA and subsequently stored at 25.5°C overnight. Synchronized embryos (8-10 hours after egg laying) were observed 24 hours after injection. N2 did not showed any major embryonic elongation defect.
†Penetrance corresponds to the percentage of embryos showing the described embryonic elongation arrest*. Other phenotypes were observed (i.e. early embryonic arrest) but are not mentioned in this table. For each genotype, $n \geq 40$ embryos.